

DEVELOPMENT OF HUMAN PBBK MODELS FOR MIXTURES: BINARY MIXTURES OF MERCURY/ SELENIUM, AND LEAD/SELENIUM

Maza, D. D* and Ojo, J. O

Nutrition & Health Related Research Laboratory, Department of Physics and Engineering Physics,
Obafemi Awolowo University, Ile-Ife, Nigeria

*Corresponding Author: danjumamaza@gmail.com

(Received 6th Aug., 2016; Accepted: 26th Sept., 2016)

ABSTRACT

Physiologically-based biokinetic models have been developed for predicting simultaneously the Absorption, Distribution, Metabolism and Elimination (ADME) properties of lead (Pb) and selenium (Se), and mercury (Hg) and selenium in a number of target tissues of humans. This was done for three population groups, namely, women of child bearing age (pregnant, lactating and non-pregnant-non-lactating), fetus, and infants/ children (0 -5 years of age). This was with a view to applying the model to environmental health risk assessment. For each of the elements, three independent models were developed for each population group, making a total of 9 models. These models were able to simulate reasonably the results of controlled experiments obtained from literature. The models were then integrated into binary pairs of Hg/Se and Pb/Se to facilitate viewing the interaction between mercury and selenium, and lead and selenium. Interaction among these elements affected the bioaccumulation of these elements in the respective tissues, thus, altering their partition coefficients. Alterations in the partition coefficients of these elements were modelled by incorporating in the models modification factors derived from the result of the study conducted by Ralston and Cohorts in 2008 on rats. This enabled the integrated models to simulate simultaneously the modulated concentration profiles due to the interaction of these elements. The modulated tissue concentrations were then used in a hypothetical health risk assessment of these elements. The results showed that until selenium intake was adequate or high, even low doses of mercury or lead could be considered as health risk. The results further showed that for the infant child, unless selenium intake was high, the brain was quite susceptible to mercury intoxication, even at low doses.

Keyword: Human PBBK Models, Binary Mixtures, Mercury/Selenium, Lead/Selenium.

Since Andersen *et al.* (1987) illustrated the use of physiologically-based biokinetic (PBBK) models in environmental health risk assessment with CH₂CL₂ in 1987, the use of PBBK models in environmental health risk assessment has increased tremendously, involving wide variety of chemicals (Andersen, 2003; US Air Force, 2005, US Environmental Protection Agency, 2006; Mumtaz *et al.*, 2012)

Physiologically-based biokinetic models are increasingly becoming quite useful for investigators in the field of environmental health risk assessment because they are well adapted to predict the internal dose of xenobiotics at target tissues (US Air Force, 2005; US Environmental Protection Agency, 2006). The heightened interest of investigators in PBBK modelling stems from the fact that the internal concentrations of active compounds at their target organs need to be related to the dose to which an animal or human subject has been exposed to or been administered. Reason being that, both beneficial and adverse effects produced by a chemical substance, in an

animal or human subject, are related to the free concentration of the active chemical agent at the target tissue and not the amount of chemical substance at the site of exposure or absorption. The complex nature of the relationship between tissue dose and absorbed dose, have made physiologically based biokinetic models very useful tools, and indeed tools of choice, in assessing the internal dose at target organs, for a wide variety of exposure scenarios, since biokinetic modelling determines the fate of a chemical agent in the body based on the rate of absorption, distribution and storage in tissues, metabolism, and excretion.

Furthermore, physiologically-based biokinetic models are useful in enhancing the understanding of the biological principles governing the kinetic behaviour of a wide variety of chemicals in biological systems (Andersen *et al.*, 1987; Andersen, 2003; Ruiz *et al.*, 2011; Campbell *et al.*, 2012). They have equally been useful tools in assessing the mechanisms of toxicity of chemical agents by providing better understanding of the

relationship between dose metrics and specific responses (Andersen *et al.*, 1987; Andersen, 2003). Additionally, as a result of their biological basis, physiological-based biokinetic models are capable of extrapolating across dose routes, between species, from high to low doses and across exposure scenarios.

The two principal concepts that describe how the individual chemicals in a mixture affect the toxicity of one another are additivity and interaction (Silins and Hogberg, 2011). While additivity assumes that if individual chemicals in a mixture act by the same or different modes of action, it will result in dose or effect addition, interaction assumes that the interaction between individual chemicals of a mixture affect the toxicity of one another by either synergism or antagonism.

The interaction between components of a chemical mixture have the tendency of affecting some critical physiological, biochemical or physiochemical parameters that determine their disposition, thereby altering their distribution profile. Where the changes to these critical parameters and the mechanism of interaction between these chemicals are quantitatively well understood, physiologically based biokinetic modelling provides mechanistic platform for predicting changes in target tissue doses of components of chemical mixtures (Krishnan *et al.*, 1994; Hadad and Krishnan, 1998; Hadad *et al.*, 2001). Physiologically-based biokinetic models are capable of describing quantitatively the interaction between the components of chemical mixtures by integrating these mechanistic determinants and thus enable the prediction of changes in tissue dose for various exposure scenarios. This underlines the usefulness of physiologically-based biokinetic models in mixture risk assessment.

While lead (Pb) and mercury (Hg) are known to be toxic elements, selenium (Se) has been known to mitigate their toxic effects. However, in the health risk assessment of lead and mercury, their interaction with selenium is seldom taken into consideration. There is therefore the need for models that will be capable of incorporating the interaction of these elements and predict simultaneously the absorption, distribution,

metabolism, and elimination (ADME) of lead, mercury and selenium in target tissues.

METHODS

General Description of the Models

The blood, liver, kidney, brain, fat, richly perfused tissues and slowly perfused tissues are compartments which are common to all the adult and infant models. Bone is a compartment only in the lead models, since lead is a bone-seeking element (the bulk of the body burden of lead is found in the bone). All soft tissues, besides the liver, kidney and brain are lumped together as richly perfused tissues. Likewise, all non-soft tissues besides bone (in the lead models) and bone/fat (in the mercury and selenium models) are lumped together as slowly perfused tissues. In all the models (adult, infant and foetus), the blood compartment is divided into two sub-compartments, plasma and red blood cells because of binding in the erythrocytes. Tissue volumes were estimated as percentage of body weight.

All compartments in the adult models, with the exception of the brain and bone compartments, were described by perfusion rate-limited kinetics, where movement of substances in and out of tissues is determined by blood flow to the tissues. The brain and bone, on the other hand, were described using permeation rate-limited kinetics, where movement of substances are control by diffusion into the tissues. In the infant and fetus models, however, the brain was modelled as a single compartment, since the brain-blood barrier is not fully developed. The infant and fetus brain were therefore described by perfusion rate-limited kinetics, while the adult brain was described by permeation rate-limited kinetics.

Non-pregnancy, Non-lactation Models

In the non-pregnancy, non-lactation models, all tissue volumes were allocated pre-pregnancy values and were assumed to remain constant within the period of simulation. Similarly, blood flow to the respective organs were assumed constant and were allocated the pre-pregnancy values. The tissue volumes and blood flow rates were modelled as percentages of pre-pregnancy body weight (Tables 1 and 2)

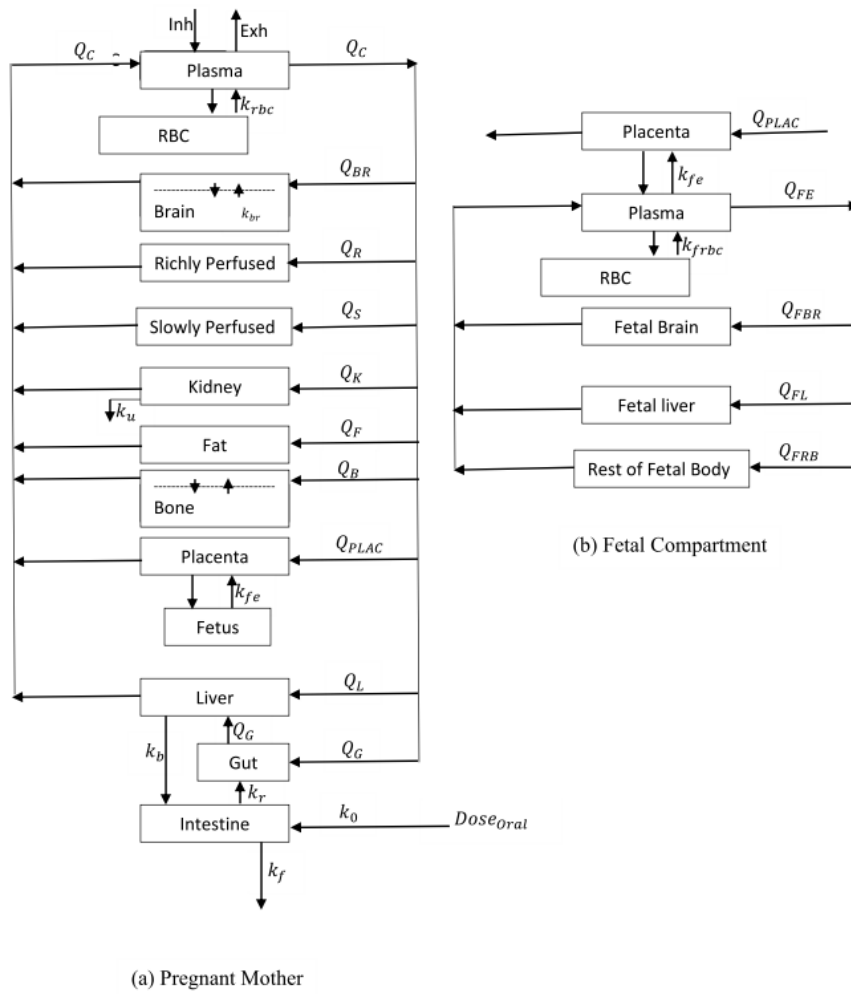


Figure 2: Pregnancy Model Sketch

Pregnancy Models

A pregnancy model (Figure 2) consists of maternal model and a fetal model. During gestation, the physiology of both the mother and fetus keep changing with gestation time. In particular, changes in the physiology of the pregnant woman is accompanied by changes to her blood volume, mammary gland, uterus and fat. As a result, these tissue organs were modeled as time dependent parameters during gestation. Although mammary gland, and uterus were not represented in the models as distinct compartments, these changes were reflected as changes to the volume of the richly perfused tissues. On the other hand, changes to fat volume during gestation is reflected as changes to the volume of the slowly perfused tissues. As a result the volume of richly perfused tissues and slowly perfused tissues were modelled as time dependent parameters in the pregnancy models.

Bone Resorption During Gestation and Lactation

During gestation, bone resorption in the pregnant mother becomes enhanced to facilitate bone formation in the fetus. Similarly, bone resorption during lactation is elevated to promote bone development in the infant. This is accompanied by the resorption of lead to the blood, since lead is a bone seeking element. In this work, bone resorption was modelled as 1.3 and 1.63 of the pre-pregnancy value during gestation and lactation respectively. Thus, Equations 1, 2, and 3 describe the kinetics of lead in the bone compartment during gestation as:

$$V_{BS} \frac{dC_{BS}}{dt} = Q_B (C_P - C_{VBS}) + B_{RRG} C_B - F_{LEAD} B_{FR} C_{BS} \quad 1$$

$$V_B \frac{dC_B}{dt} = F_{LEAD} B_{FR} C_{BS} - B_{RRG} C_B \quad 2$$

with $B_{RRG} = 1.3B_{RR}$ 3

Where B_{RR} and B_{RRG} are pre-pregnancy and gestation bone resorption rates respectively. V_{BS} and V_B are volumes of the bone-surface and bone-matrix sub-compartments respectively, Q_B is blood flow to the bone, C_{VBS} is concentration of lead in the venous blood exiting the bone compartment. C_p , C_{BS} and C_B are the concentration of lead in the plasma, bone-surface, and bone-matrix sub-compartments respectively, F_{LEAD} is the fractional clearance of lead from plasma into forming bone, while B_{FR} is the bone formation rate.

Lactation Models

A lactation model is an integration of a maternal and an infant model, to simulate the ADME of both mother and infant child, simultaneously. All tissue volumes and blood flow rates in the maternal model, except mammary gland and fat, were modeled as constant fractions of body weight. On the other hand, the volume and blood flow rates of mammary gland and fat were modelled as time dependent parameters.

Infant Parameters

All tissue volumes and blood flow rates in the infant models were modelled as time dependent parameters. However, they were modelled as

constant fractions (same as the adult fractional body weight) of the infant body weight, BWN , which is described by Equation 4 (Yoon *et al.*, 2011)

$$BWN = 13.64(1 - \exp(1 - 0.055AGE_m)) + BWN_0 \quad 4$$

Where, AGE_m is the infant's age in months, and BWN_0 is the infant's body weight at birth in kg.

Model Evaluation

Model evaluation was carried out using the results of controlled studies obtained from literature (O'Flaherty, 1993; Gearheart *et al.*, 1995; Shipp *et al.*, 2000; Bugel *et al.*, 2008). The experimental data of these controlled studies were not available in the published work of these authors, however, data were extracted from the graphical presentation of these works, using a software known as Graph Data Extractor. The evaluations were carried out primarily for the individual models. Model simulations and extracted experimental data were presented on the same graph for ease of comparison. Data from two subjects were used to evaluate the lead and the mercury models. On the other hand, the data used to evaluate the selenium models is the average for 12 subjects.

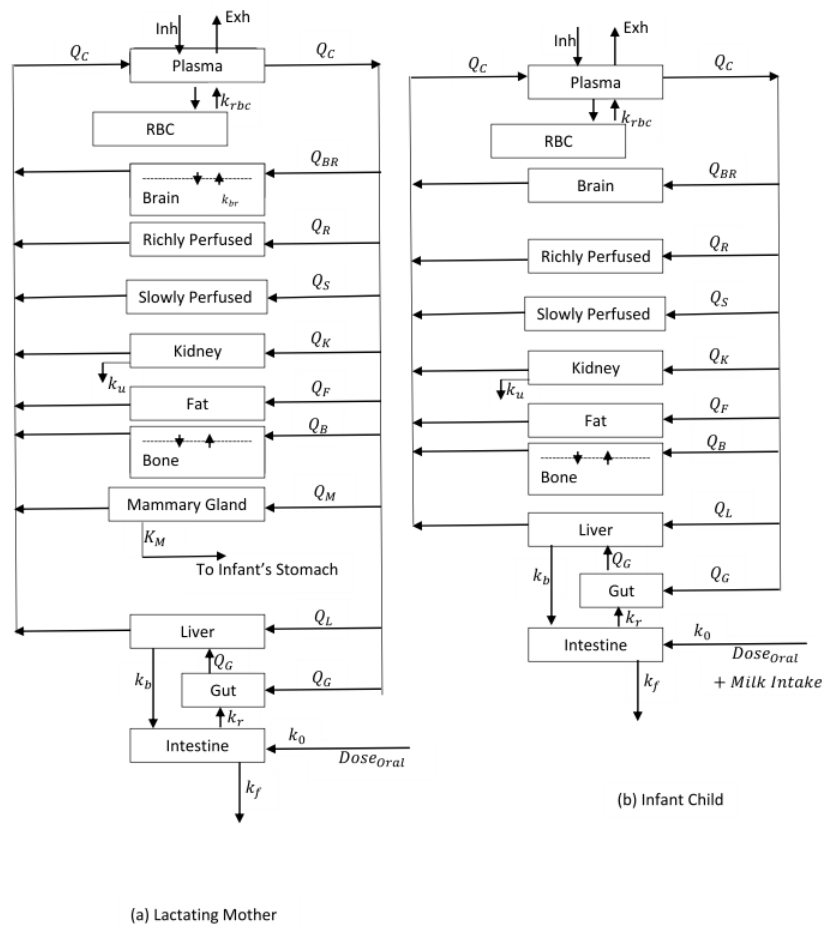


Figure 3: Lactation Model Sketch

Lead Models Evaluation

Figures 4 and 5 are graphs displaying the concentration measurements and model simulations of two human subjects (Subject A and Subject B) who participated in a study conducted by Rabinowitz and co-researchers in 1976 (O'Flaherty, 1993). The subjects were given 50 μg of stable isotope of lead per day through drinking water for the period of exposure (104 days for subject A and 82 days for subject B). The dotted points are concentration measurements, while the solid curves are the model simulations for the subjects.

Although the weight, gender, and age of the subjects were not specified, the pregnancy model simulation (Figure 4) for a 25-year old pregnant woman, weighing 60 kg gave a good description of the data of subject A. While for subject B, the pregnancy model simulation (Figure 5), for a 30-year old pregnant woman weighing 65 kg, gave a good description of the data of the subject, although the other two independent models (non-pregnancy, non-lactation and lactation models) describe fairly well the kinetics of lead in the blood of the subject.

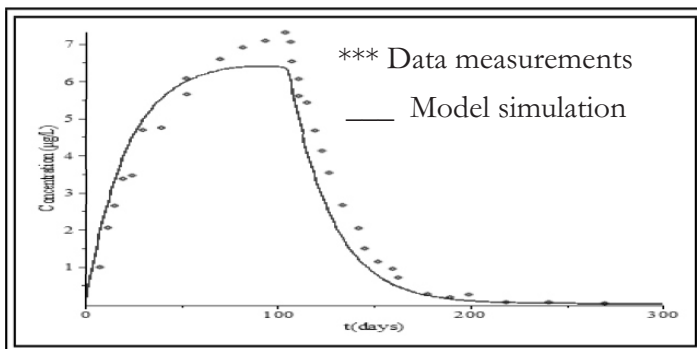


Figure 4: Lead Models Evaluation (With Individual Element Models) Graphs 1 (Subject A. The subject was given 50 μg of stable isotope of lead per day through drinking water for 104 days.

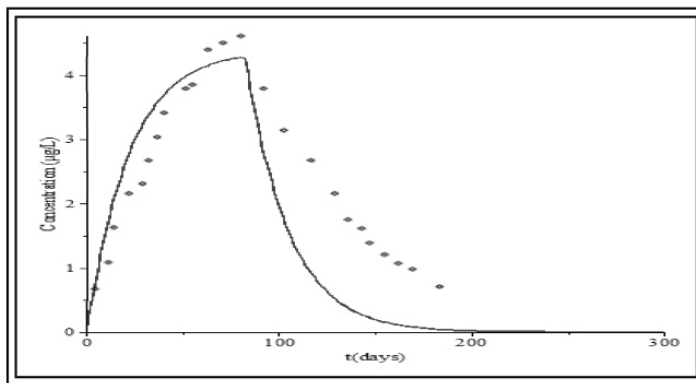


Figure 5: Lead Models Evaluation (With Individual Element Models) Graphs 2 (Subject B. The subject was given 50 μg of stable isotope of lead per day through drinking water for 82 days

Mercury Models Evaluation

The ability of the mercury models to provide a reasonable description of MeHg kinetics in the blood of human subjects is illustrated in Figures 6 and 7. The dotted data points are the average measurements for at least five subjects who participated in a controlled study of chronic ingestion of MeHg through fish intake at doses of 3.69 μg and 2.69 μg of MeHg /Kg/day

respectively for approximately three months in a study carried out by Sherlock and co-workers in 1984 (data from Gearheart *et al.*, 1995 and Shipp *et al.*, 2000), while the solid curves are the model simulations. The simulations in Figures 6 and 7, for a non-pregnant, non-lactating woman, provided a reasonable description of the kinetics of MeHg in the whole blood of the human subjects at the two doses used for this evaluation.

Figure 6: Mercury Models Evaluation (With Individual Element Models) Graphs 1 (Subjects ingested MeHg through fish consumption at doses of 3.69 $\mu\text{g}/\text{Kg}/\text{day}$ for approximately three months. The dotted points are concentration measurements, while the solid curves are the model simulation.

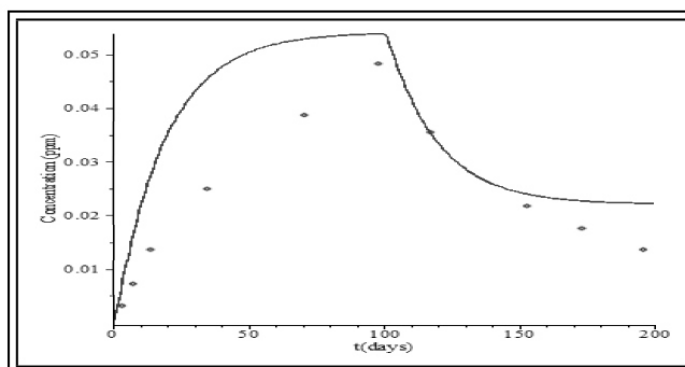
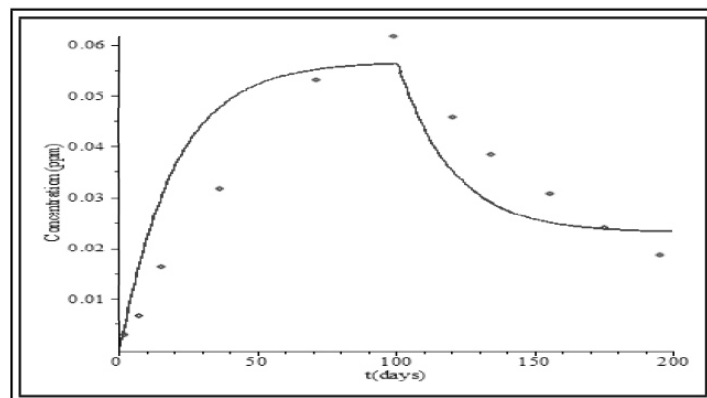


Figure 7: Mercury Models Evaluation (With Individual Element Models) Graphs 2 (Subjects ingested MeHg through fish consumption at doses of 2.69 $\mu\text{g}/\text{Kg}/\text{day}$ for approximately three months. The dotted points are concentration measurements, while the solid curves are the model simulation).

Selenium Models Evaluation

Figure 8 displays the ability of the selenium models to describe the kinetics of selenium in the plasma of human subjects. The data points represent the mean plasma concentration ($\mu\text{g/L}$) of ^{77}Se isotope given to 12 human volunteers with high habitual intake of selenium. In a study carried

out by Bugel *et al.*, 2008, the twelve volunteers were given a single oral dose of $327\mu\text{g}$ of ^{77}Se isotope as selenium yeast, with a light meal after an overnight fast. The solid curve represents the model simulation. This simulation described reasonably, the kinetics of selenium in the plasma of the human volunteers.

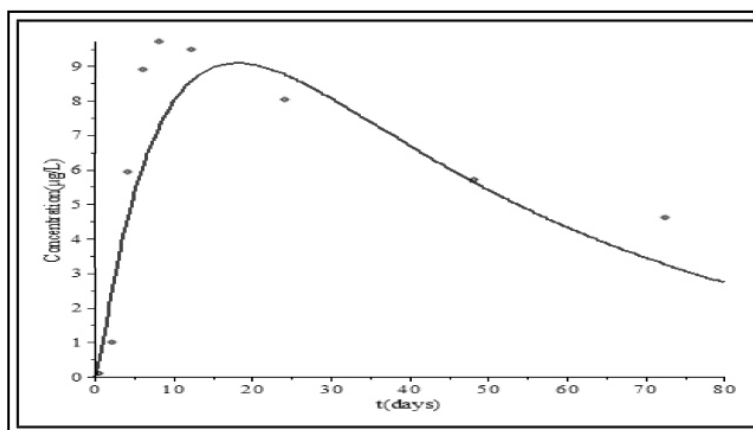


Figure 8: Selenium Models Evaluation Graph

Model Integration

The independent models that were developed were integrated to provide a platform for viewing the interaction between the elements, mercury and selenium, and lead and selenium. Figure 9 shows the framework of the integration of the binary mixtures. The models were integrated in pairs (i.e. Pb/Se and Hg/Se), to provide a platform for viewing the interaction between Hg and Se, and between Pb and Se.

Interaction was modelled primarily for dietary oral ingestion, due to availability of data. Modelling the integrations was predicated on the fact that both mercury and lead have very high affinity ($\approx 10^{45}$) for selenium (Curvin-Aralar and Furness, 1991; Raymond and Ralston, 2004; Ralston, 2008; Flora *et al.*, 2008). As a result, both of these elements form insoluble complexes with selenium (i.e. $\text{Pb} + \text{Se} \rightarrow \text{Pb-S}$ (complex), and $\text{Hg} + \text{Se} \rightarrow \text{Hg-Se}$ (complex)).

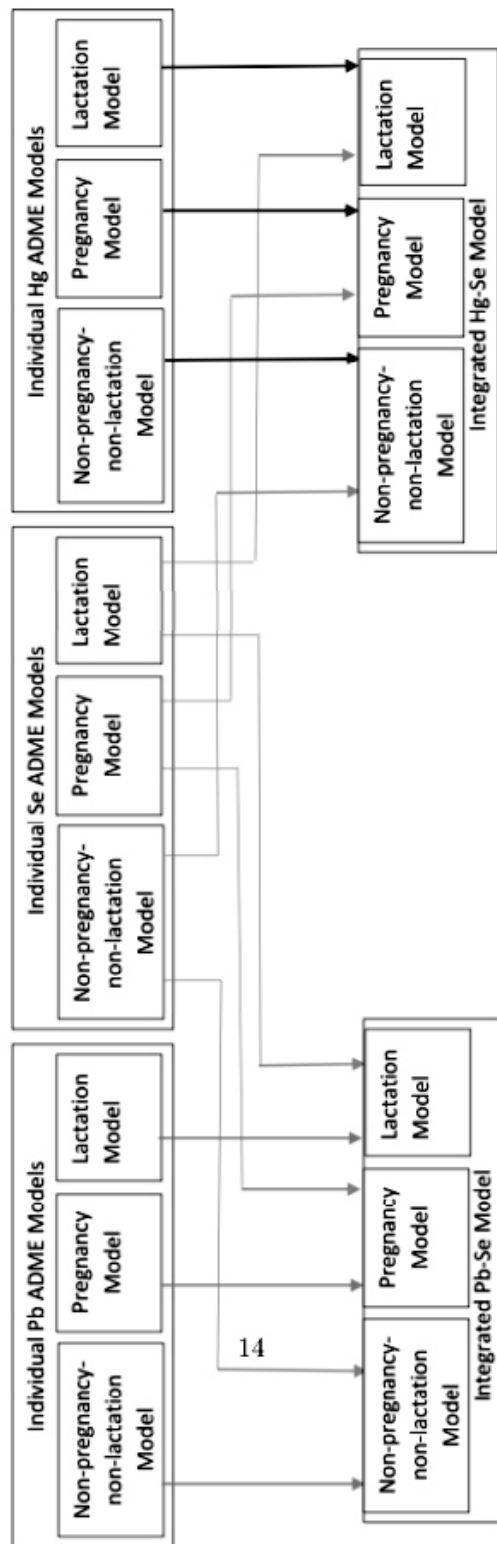


Figure 9: Framework for the Integration of the Binary Mixtures of Hg/Se and Pb/Se

Because the complexes formed are insoluble, the retention of these elements in various tissues are affected, altering their partition coefficients in the respective organs (Krishnan *et al.*, 1994). The

concentration of the chemical substance in the venous blood, c_{VT} , exiting a given tissue, T is now modified as

$$C_{VT} = \frac{C_T}{\alpha_T P_T} \quad 5$$

Where α_T is the modification factor for the partition coefficient. C_T and P_T retain their usual meaning. This leads to modifications in the mass balance ordinary differential equations. Consequently, the modified mass balance equation for tissues described by perfusion rate-limited kinetics is given by

$$V_T \frac{dC_T}{dt} = Q_T (C_P - \frac{C_T}{\alpha_T P_T}) \quad 6$$

Similarly, the modified mass balance equations for tissues described by permeation rate-limited kinetics are given as

$$V_{TS} \frac{dC_{TS}}{dt} = Q_T (C_P - C_{TS}) - PAF (C_{TS} - \frac{C_{TD}}{\alpha_T P_T}) \quad 7$$

and

$$V_{TD} \frac{dC_{TD}}{dt} = PAF (C_{TS} - \frac{C_{TD}}{\alpha_T P_T}) \quad 8$$

The modification factors were estimated using data from animal studies (Ralston and Raymond, 2008; Ralston *et al.*, 2008). The animals (rats) used in these studies were dosed in proportion to their body weight, which enables scaling to human body weight. Furthermore, although the tissue organs studied by Ralston *et al.*, (2008) were blood, liver, kidney and brain, modification factors for other organs not covered by their work were estimated by allocating the same modification factor to physiologically similar tissues. To model the interactions, doses were categorized as shown in Table 3. The categorization was used to implement a switching system in the code, similar to what is obtainable in digital electronics. For mercury and Lead, low and high dose regimes were assigned values of 0 and 1 respectively, while low, adequate and high dose regimes for selenium were assigned values of 0, 1 and 2 respectively. For the models to be able to provide a platform for viewing ADME properties when there is an interaction and when there is no interaction, a variable M was introduced. The variable M assumes the value 0 when interactions are not modelled, and the value 1 when interactions

modelled. If we use Hg, Pb and Se as symbols to represent the respective dose states of the elements then Hg and Pb can assume values 0 and 1, corresponding to low and high dose states of mercury, lead respectively. Similarly Se can assume values 0, 1 and 2, corresponding to low, adequate and high dose states of selenium respectively.

Logic circuit (Figure 10) was then designed to facilitate the switching system for modelling the interactions. Truth tables were then constructed for each tissue compartment, based on the work of Ralston *et al.*, (2008), to facilitate the development of the code that modelled the modifications to the partition coefficients.

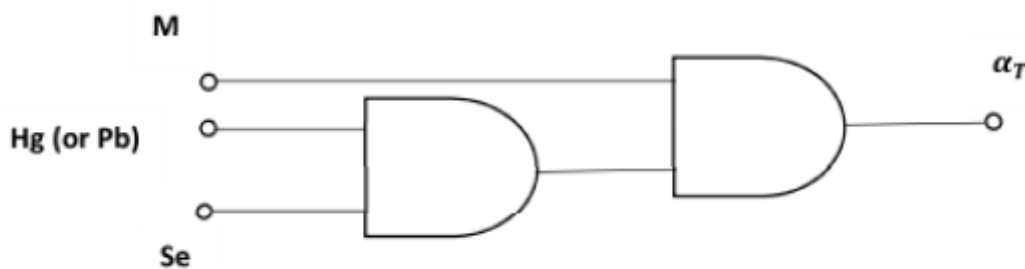


Figure 10: Logic Circuit for Hg/Se and Pb/Se Models

Table 3: Dose Categorization

Hg Dose		Pb Dose		Se Dose	
($\mu\text{mols/Kg}$)		($\mu\text{mols/Kg}$)		($\mu\text{mols/Kg}$)	
≤ 0.5	Low	≤ 0.5	Low	≤ 1.0	Low
≥ 0.5	High	≥ 0.5	High	$\geq 1.0 \leq 5.0$	Adequate
				> 5.0	High

Applying the Integrated Models in Risk Assessment

Hypothesis

To apply the integrated models in risk assessment, it was hypothesized that the Health Risk Index (HRI) associated with Hg and Pb are respectively the Hg-to-Se and Pb-to-Se molar ratios. The use of Hg-to-Se molar ratio as the health risk index, in case of mercury toxicity, was proposed as early as 1972 by Ganther and collaborators (e.g. Zhang, 2014). However, this proposal was given little attention because the specific underlying mechanisms of toxicity of mercury were not understood until recently.

However, there is growing evidence that the toxicity of mercury results from mercury-induced selenium deficiency occasioned by Hg-Se complex formation (Curvin-Aralar and Furness, 1991; Raymond and Ralston, 2004; Ralston, 2008; Flora *et al.*, 2008). The results of animal studies (Ralston and Raymond, 2008; Ralston *et al.*, 2008) indicate that using the Hg-to-Se molar ratio

instead of the Hg concentration alone, gives a more realistic estimate of the toxicity of mercury in the brain, liver and kidney.

In this work, the Hg-to-Se molar ratio is being used as the health risk index of mercury in the respective tissues. Similarly, due to similarities in the interaction between mercury and selenium and between lead and selenium, the Pb-to-Se molar ratio is being used as the health risk index of lead in the respective tissues. Thus, the health risk index of mercury, HRI_{HgT} , in a given tissue is estimated as

$$HRI_{HgT} = \frac{C_{HgT}}{C_{SeT}} \quad 9$$

Where C_{HgT} and C_{SeT} are the molar concentrations of Hg and Se in tissue T respectively. Similarly, the health risk index of lead, HRI_{PbT} , in a given tissue is estimated by

$$HRI_{PbT} = \frac{C_{PbT}}{C_{SeT}} \quad 10$$

Where C_{pBT} is the molar concentration of Pb in tissue T.

RESULTS AND DISCUSSION

Viewing the Interaction between the Elements

The integration of the individual models provides a platform for viewing the effect of the interaction between these elements on their respective tissue concentrations. Under different co-exposure scenarios, the interaction of mercury with selenium, lead with selenium were viewed. All simulation were for continues exposure for a period of 100 days, except for the pregnancy models simulations which were for 270 days

Interaction of Mercury with Selenium

Depicted in Figures 11 and 12 are graphs illustrating the modulating effect that the interaction between mercury and selenium have on their respective tissue concentrations in a pregnant woman and her fetus, following continuous co-exposure to low doses of both mercury and selenium (0.241 $\mu\text{mol/Kg/day}$ of mercury and 0.380 $\mu\text{mol/Kg/day}$ of selenium).

Figure 11 shows that the predicted concentration of mercury in the liver of the pregnant woman and her fetus increased by a factor of 2.01 when interaction was modelled. This is consistent with an increase, by a factor of 2.016, found in rats co-exposed to mercury and selenium under similar conditions (Ralston *et al.*, 2008). Similarly,

following the interaction between mercury and selenium, the simulated concentration of mercury in the kidney, richly perfused tissues, and slowly perfused tissues of the pregnant woman were modified by factors of 0.911, 0.912, and 0.90 respectively which are in close agreement with the modulating factor of 0.93 obtained in rats following co-exposure to mercury and selenium under similar conditions. While the concentration in the brain of the fetus was modified by a factor of 0.893.

On the other hand, Figure 12 shows that the concentration of selenium in the liver of the pregnant woman following the continuous co-exposure to low doses of mercury and selenium (0.231 $\mu\text{mol/Kg/day}$ of mercury and 0.380 $\mu\text{mol/Kg/day}$ of selenium), was modified by a factor of about 0.032, which is in good agreement with the factor of 0.03 found in rats co-exposed under similar conditions. While the simulated concentration of selenium in the kidney, richly perfused tissues, and slowly perfused tissues were modulated by factors of 0.23, 0.23, and 0.20 respectively, which are equally in good agreement with a factor of 0.214 found in rats co-exposed to mercury and selenium under similar conditions. Given the same co-exposure scenarios (0.231 $\mu\text{mol/Kg/day}$ of mercury and 0.380 $\mu\text{mol/Kg/day}$ of selenium), it suffices to say that the same trend was observed in the non-pregnancy, non-lactation and lactation model simulations.

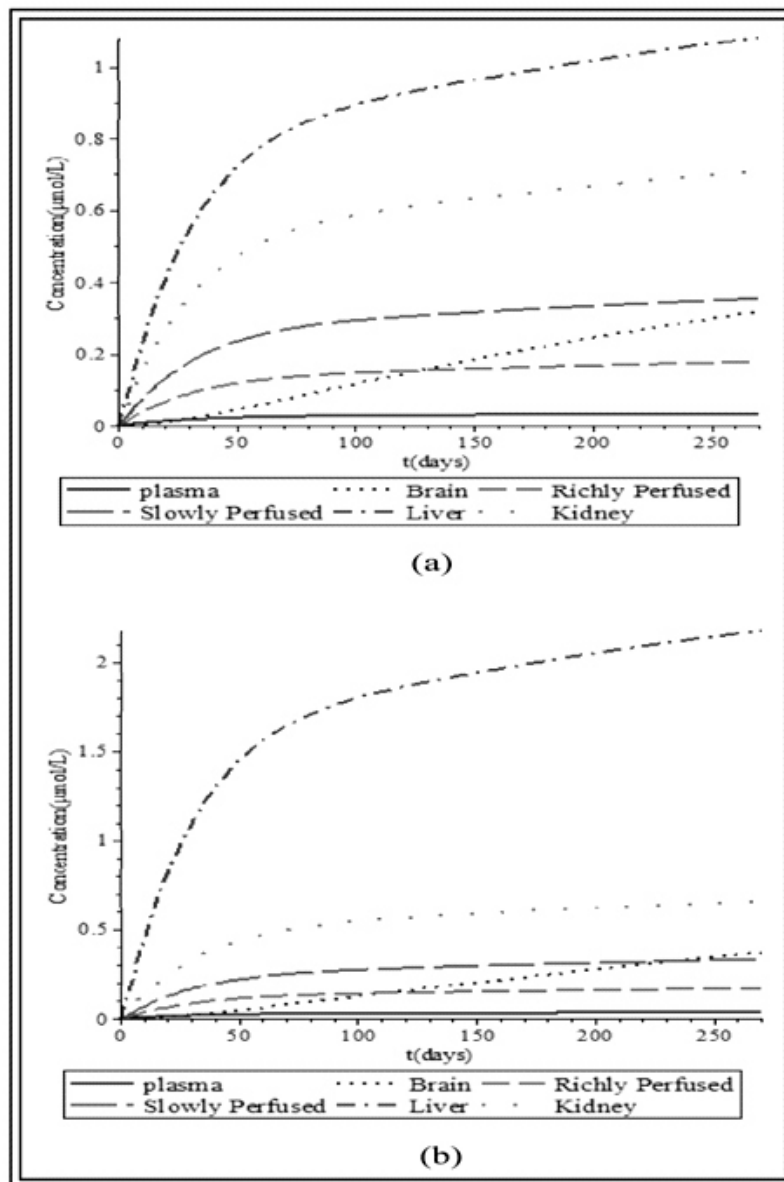


Figure 11: Effect of the Interaction between Mercury and Selenium on Mercury Concentration in a Pregnant Woman: Co-exposure to Low Doses of Both Mercury and Selenium, i.e. $0.231 \mu\text{mol/Kg/day}$ of Mercury and $0.380 \mu\text{mol/Kg/day}$ of Selenium. (a) Concentration profiles Without Interaction (b) Modulated Concentration Profiles Due to Interaction.

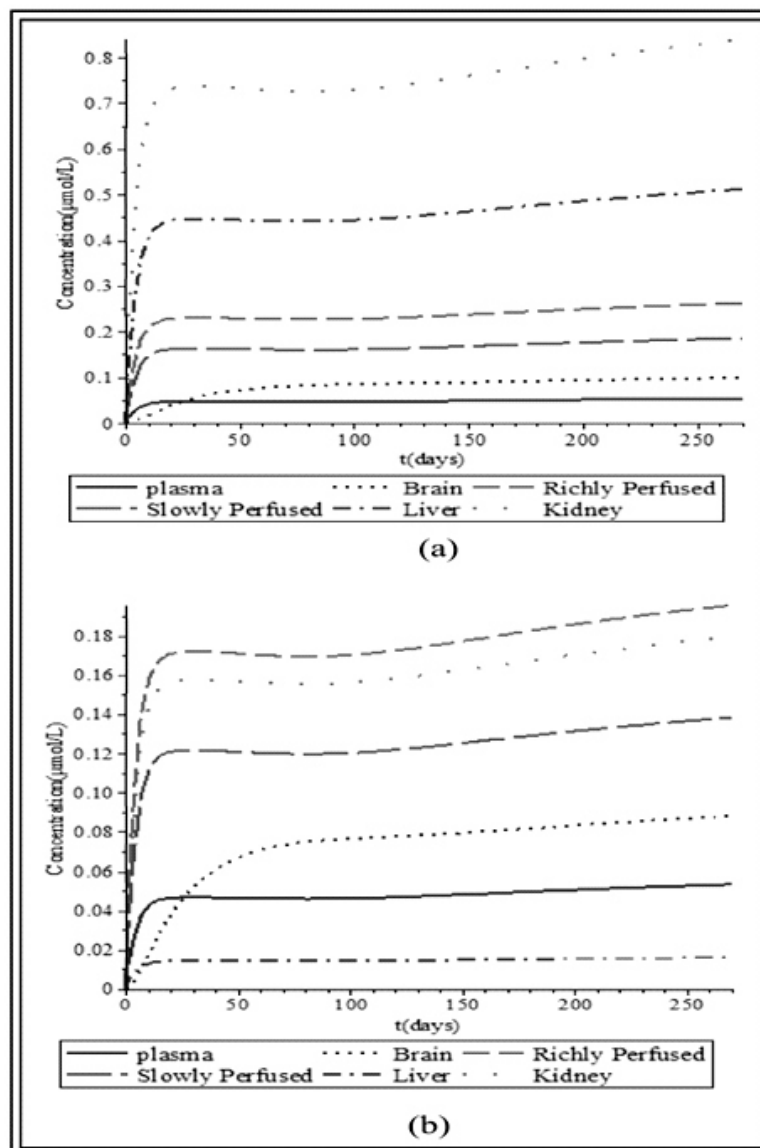


Figure 12: Effect of the Interaction between Mercury and Selenium on Selenium Concentration in a Pregnant Woman: Co-exposure to Low Doses of Both Mercury and Selenium. i.e. $0.231 \mu\text{mol/Kg/day}$ of Mercury and $0.380 \mu\text{mol/Kg/day}$ of Selenium. (a) Concentration profiles Without Interaction (b) Modulated Concentration Profiles Due to Interaction.

Figures 13 and 14 are graphs depicting the effect of the interaction between mercury and selenium on their respective concentrations in different tissues, following the co-exposure of a non-pregnant, non-lactating woman to low dose of mercury and high dose selenium ($0.231 \mu\text{mol/Kg/day}$ of mercury and $10.0 \mu\text{mol/Kg/day}$ of selenium). Figure 13 shows that the mercury concentration in the liver and kidney were modulated by factors of 1.30 and 0.82 respectively. In the same vein, Figure 14 shows that the concentration of selenium in the liver and kidney were respectively modulated by factors of

1.34 and 1.52. All these factors are in good agreement with what was obtained in rats co-exposed under similar conditions (Ralston *et al.* 2008). The same trend can be observed in the pregnancy and lactation model simulations.

Interaction of Lead with Selenium

The concentration profiles of both lead and selenium were modified by factors similar to those obtained for mercury and selenium interaction. The reason for this is that the interaction between lead and selenium was modelled based on the assumption that selenium does not really

"distinguish" between lead and selenium when interacting with them.

Applying the Integrated Hg/Se and Pb/Se Models in Health Risk Assessment

The ability of the Hg/Se and Pb/Se integrated models to estimate the health risk posed to individual tissues as a result of mercury or lead contamination in the presence of varying doses of selenium are here in demonstrated and discussed.

It has been shown that the health risk index due to mercury in a given tissue, T, is estimated by Hg-to-Se molar ratio, while the health risk index due to lead in a given tissue is the Pb-to-Se molar ratio. Figures 15 to 18 are simulations from Hg/Se integrated models, showing the health risk index in respective tissues due to low dose of mercury and varying doses of selenium, Figure 19 shows the health risk indices in tissues of a fetus co-exposed to low doses of both lead and selenium.

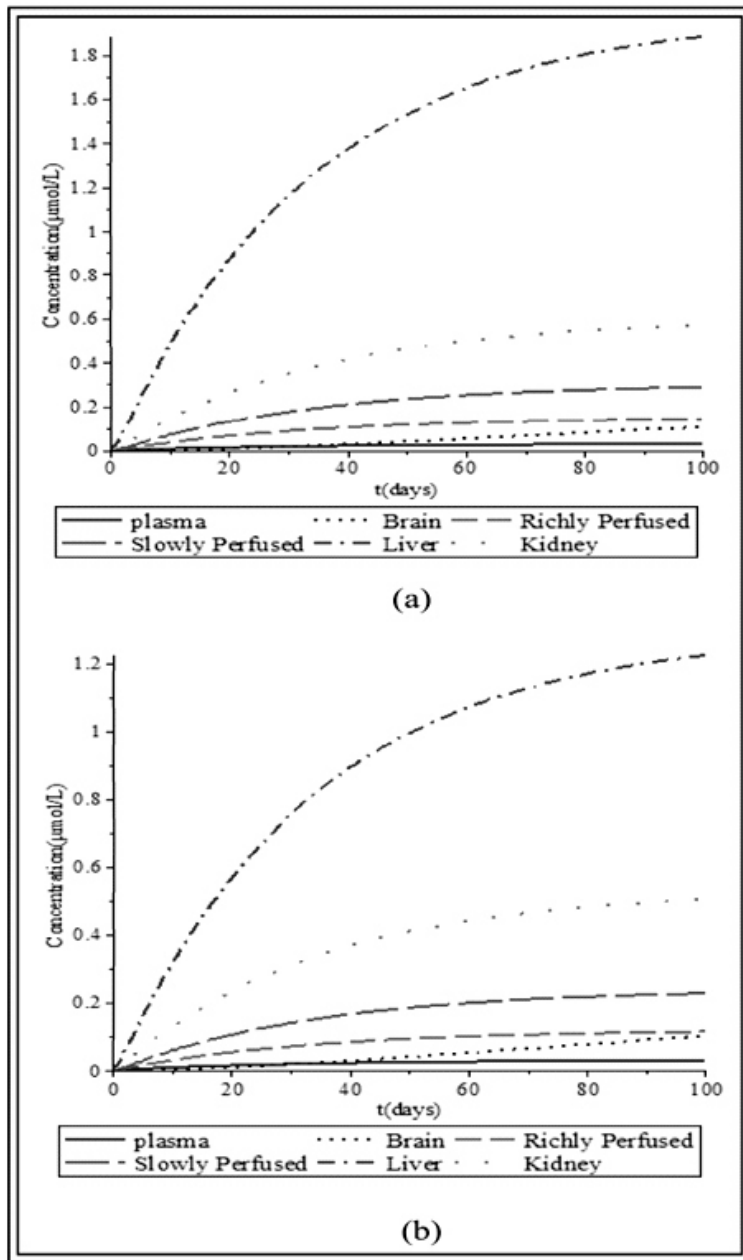


Figure 13: Effect of the Interaction between Mercury and Selenium on Mercury Concentration in a Non-pregnant, non-lactating Woman: Low Dose of Mercury and High Dose of Selenium. i.e. 0.231 µmol/Kg/day of Mercury and 10.0 µmol/Kg/day of Selenium. (a) Concentration Profiles Without Interaction (b) Modulated Concentration Profiles Due to Interaction.

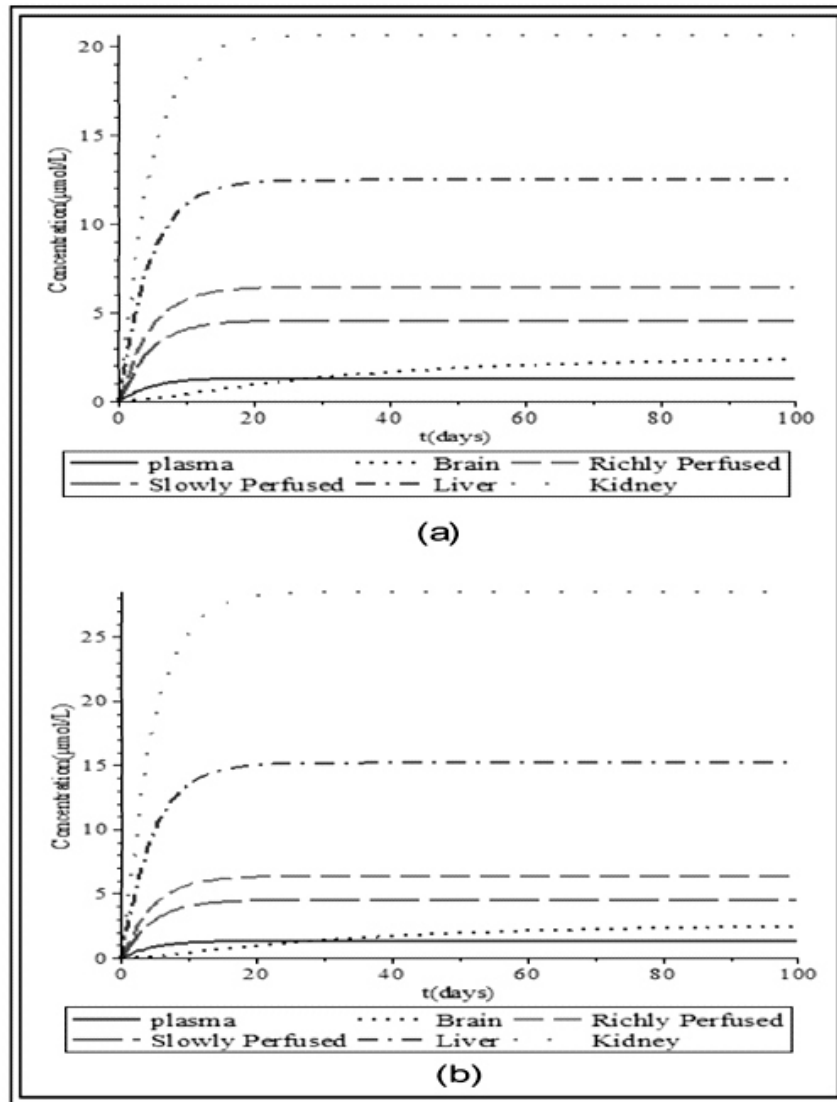


Figure 14: Effect of the Interaction between Mercury and Selenium on Mercury Concentration in a Lactating Woman: High Dose of Mercury and Low Dose of Selenium. i.e. $10.0 \mu\text{mol/Kg/day}$ of Mercury and $0.38 \mu\text{mol/Kg/day}$ of Selenium. (a) Concentration Profiles Without Interaction (b) Modulated Concentration Profiles Due to Interaction.

From Figure 15a, for low dose of mercury and low dose of selenium, the health risk indices in the plasma, brain and kidney of a non-pregnant, non-lactating woman remained low within the period of simulation, while the health risk index in the liver is significantly high. On the other hand, the simulation in Figure 15b shows that in the presence of adequate selenium intake, the health

risk index due to mercury in all tissues are below 1.0. Furthermore, Figure 15c shows that increase of selenium intake to high dose, reduces the health risk index to all tissues below 0.1, which is very low. Thus, until selenium intake is adequate or high, even low doses of mercury can be considered as a health risk.

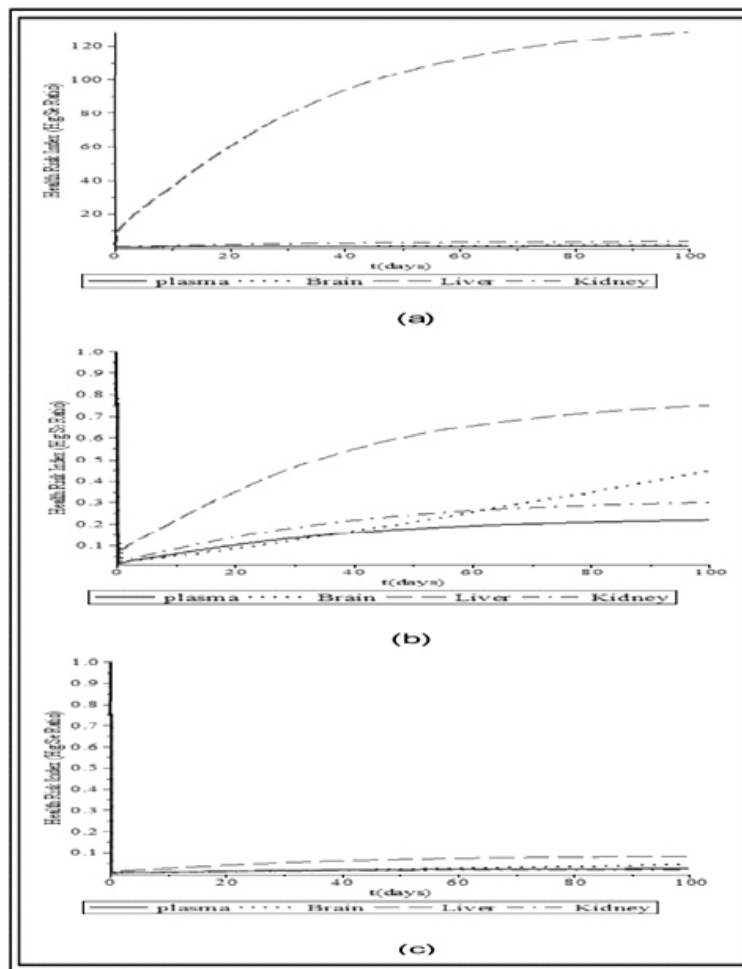


Figure 15: Health Risk Index as a Function of Time in Tissues of a Non-pregnant, non-lactating Woman Co-exposed to Low Dose of Mercury and Varying Doses of Selenium. (a) Low Dose of Mercury ($0.231 \mu\text{mol/Kg/day}$) and Low Dose of Selenium ($0.380 \mu\text{mol/Kg/day}$) (b) Low Dose of Mercury ($0.231 \mu\text{mol/Kg/day}$) and Adequate Dose of Selenium ($1 \mu\text{mol/Kg/day}$) (c) Low Dose of Mercury ($0.231 \mu\text{mol/Kg/day}$) and High Dose of Selenium ($10 \mu\text{mol/Kg/day}$).

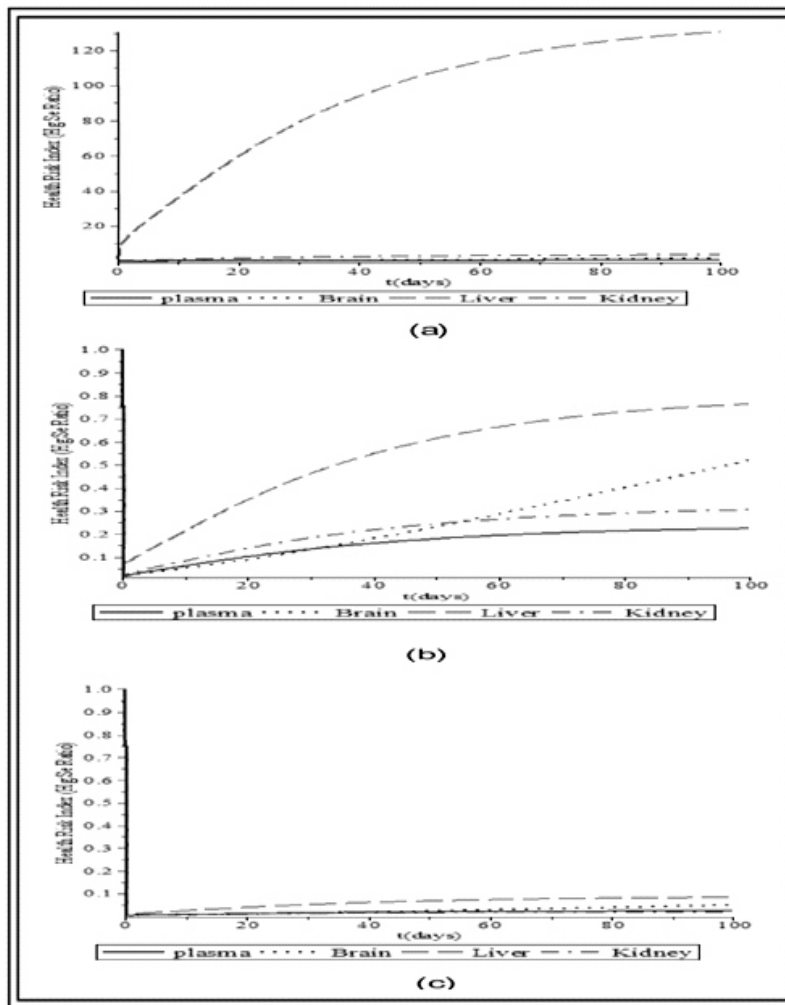


Figure 16: Health Risk Index as a Function of Time in Tissues of a Pregnant Woman Co-exposed to Low Dose of Mercury and Varying Doses of Selenium. (a) Low Dose of Mercury ($0.231 \mu\text{mol/Kg/day}$) and Low Dose of Selenium ($0.380 \mu\text{mol/Kg/day}$) (b) Low Dose of Mercury ($0.231 \mu\text{mol/Kg/day}$) and Adequate Dose of Selenium ($1 \mu\text{mol/Kg/day}$) (c) Low Dose of Mercury ($0.231 \mu\text{mol/Kg/day}$) and High Dose of Selenium ($10 \mu\text{mol/Kg/day}$).

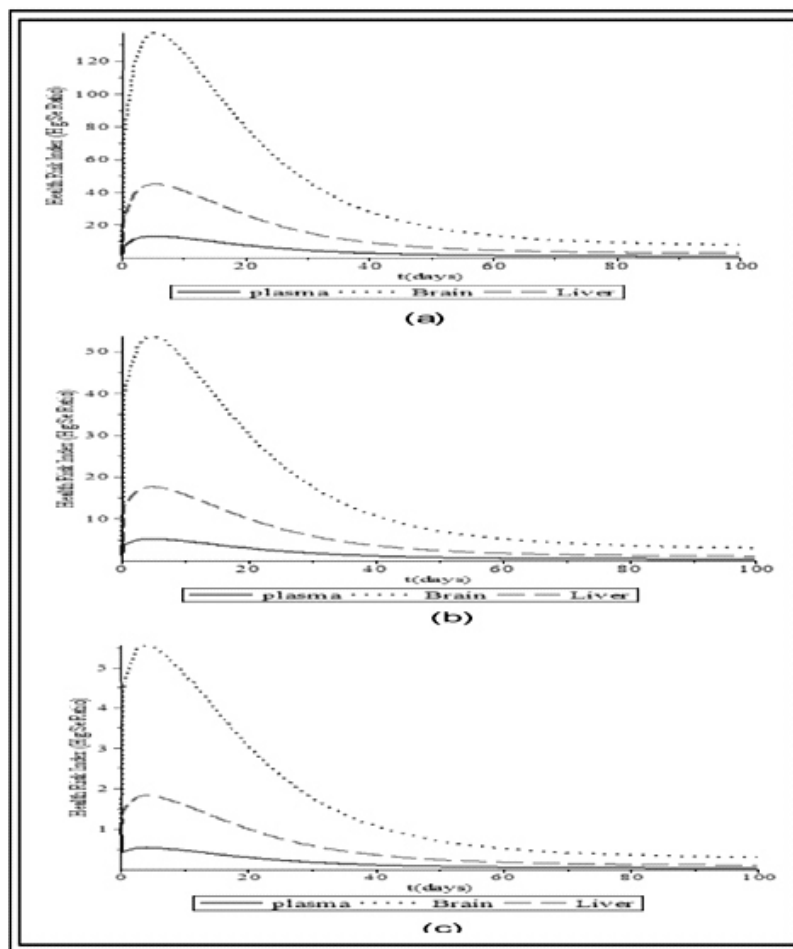


Figure 17: Health Risk Index as a Function of Time in Tissues of a fetus Co-exposed to Low Dose of Mercury and Varying Doses of Selenium. (a) Low Dose of Mercury ($0.231\mu\text{mol/Kg/day}$) and Low Dose of Selenium ($0.380\mu\text{mol/Kg/day}$) (b) Low Dose of Mercury ($0.231\mu\text{mol/Kg/day}$) and Adequate Dose of Selenium ($1\mu\text{mol/Kg/day}$) (c) Low Dose of Mercury ($0.231\mu\text{mol/Kg/day}$) and High Dose of Selenium ($10\mu\text{mol/Kg/day}$).

The simulations in Figures 16 and 17 depict the health risk index estimation in tissues of a pregnant woman and her fetus respectively, using the integrated Hg/Se pregnancy model. The health risk index in tissues of the pregnant woman (Figure 15) are similar to that of Non-pregnant, non-lactating woman (Figure 16). However, the simulations in Figure 17, depicting the health risk index in tissues of the fetus, shows that all tissues of the fetus are quite vulnerable if the mother is exposed to even low doses of mercury, unless selenium intake is high. This is particularly so in the first trimester.

For the lactating mother and her infant child, the health risk indices in the tissues of the lactating woman follows that of the non-pregnant, non-lactating woman. While Figure 18 shows that for

low doses of mercury, the health risk index in the brain of the infant remains above 1.0 at equilibrium even when selenium intake is considered adequate. This shows that the brain of the infant child is quite susceptible to mercury intoxication even at low doses, unless selenium intake is high. This most likely reflects the fact that the blood-brain barrier is not yet fully developed at this stage.

The health risk indices due to exposure to low doses of lead in the tissues of a non-pregnant, non-lactating woman, pregnant woman, and lactating woman, follows the same pattern as the health risk indices due to mercury. However, the health risk index in all tissues of the fetus (Figure 19) appear quite low even with low selenium intake and bone resorption being modelled at 30 percent

increase during gestation. This suggest that the fetus may not be in any serious danger provided the lead dose to the mother is low.

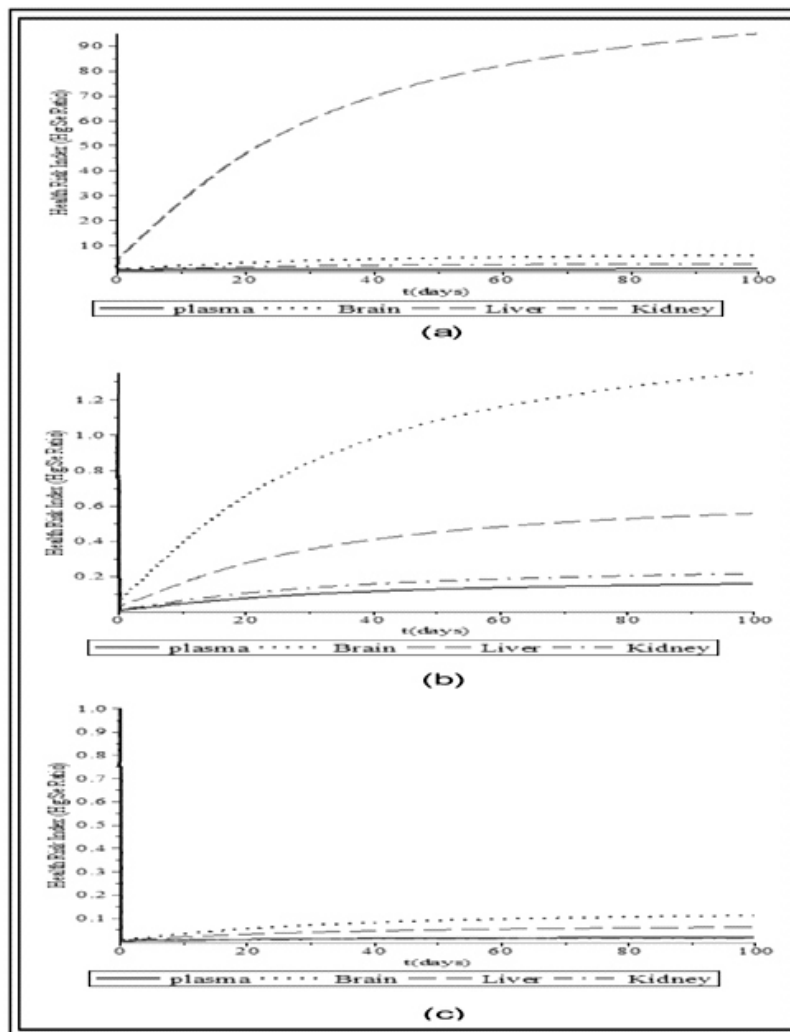


Figure 18: Health Risk Index as a Function of Time in Tissues of an Infant Co-exposed to Low Dose of Mercury and Varying Doses of Selenium. (a) Low Dose of Mercury (0.231 $\mu\text{mol/Kg/day}$) and Low Dose of Selenium (0.380 $\mu\text{mol/Kg/day}$) (b) Low Dose of Mercury (0.231 $\mu\text{mol/Kg/day}$) and Adequate Dose of Selenium (1 $\mu\text{mol/Kg/day}$) (c) Low Dose of Mercury (0.231 $\mu\text{mol/Kg/day}$) and High Dose of Selenium (10 $\mu\text{mol/Kg/day}$).

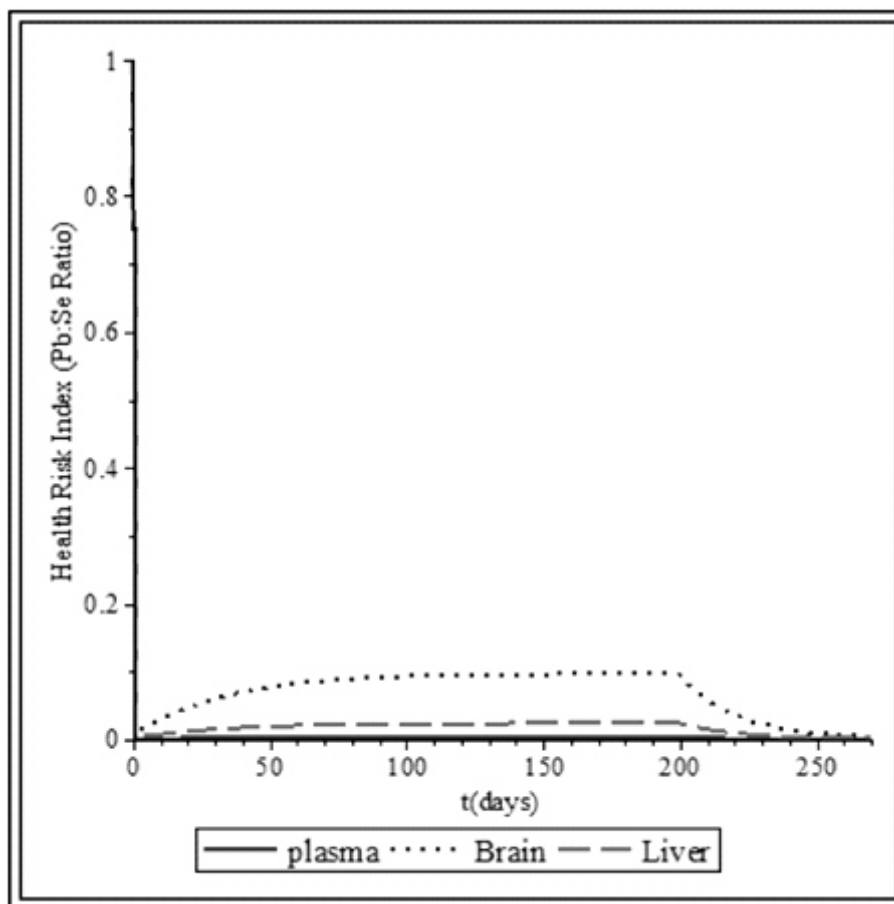


Figure 19: Health Risk Index as a Function of Time in Tissues of a Fetus Co-exposed to Low Dose of Lead ($0.241 \mu\text{mol/Kg/day}$) and Low Dose of Selenium ($0.380 \mu\text{mol/Kg/day}$).

CONCLUSION

This study has resulted in the development of physiologically based biokinetic models for the binary mixtures of lead and selenium, and mercury and selenium. Preparatory to the development of the models for mixtures, individual physiologically-based biokinetic models were developed for lead, mercury and selenium and evaluated. The result of the evaluation shows that these individual models simulate reasonably well the result of controlled experiments obtained from literature.

The binary mixture models developed are capable of simulating simultaneously, under various co-exposure scenarios, the absorption, distribution metabolism and elimination (ADME) properties of these elements in a number of tissues of three population groups of humans (i.e., pregnant women and their fetuses, lactating women and their infant children, and non-pregnant, non-lactating women). These models have also

demonstrated their ability to be useful tools in the health risk assessment of the mixture of these elements.

When applied in hypothetical health risk assessment, in various co-exposure scenarios, the binary mixture models were capable of estimating the health risk index to individual tissue organs. In the course of the hypothetical health risk assessment, it was observed that in the absence of adequate selenium intake, even low doses of lead or mercury could constitute significant health risk to some organs. Thus, the adequacy or inadequacy of selenium is what determines whether a given dose of lead or mercury poses a significant health risk to some organs or not. It was further observed that all tissues of the fetus are quite susceptible to mercury intoxication if the mother is exposed to even low doses of mercury, unless selenium intake is high, particularly in the first trimester. However, provided the lead dose to the mother is low, the tissues of the fetus may not be in any great danger.

Additionally, it was observed that for the infant child, the brain is quite susceptible to mercury intoxication even at low doses, unless selenium intake is high.

REFERENCES

- Andersen, M. E. 2003. Toxicokinetic modelling and its applications in chemical risk. *Toxicology Letters*, 138: 9-27.
- Andersen, M. E., Clewell, H. J., Gargas, M. L., Smith, F. A., and Ruiz, R. H. 1987. Physiologically based pharmacokinetics and the risk assessment process for methylene chloride. *Toxicology and Applied Pharmacology*, 87:185-205.
- Bugel, S. G., Larsen, E. H., Sloth, J. J., Flytjie, K., Overvad, K., Steenberg, L. C., and Moesgaard, S. 2008. Absorption, excretion, and retention of selenium from a high selenium yeast in men with a high intake of selenium. *Food and Nutrition Research* 10.3402/fnr.v52.10.1642.
- Campbell Jr, J. L., Clewell, R. A., Gentry, P. R., Andersen, M. E., and Clewell III, H. J. 2012. Physiologically based pharmacokinetic/toxicokinetic modelling. In *Computational Toxicology*, Chapter 18. Springer Science + Business Media, LLC 2012.
- Curvin-Aralar, M. L. A. and Furness, R. W. 1991. Mercury and selenium interaction: A review. *Ecotoxicology and Environmental Safety*, 21:348-364.
- Flora, S. J. S., Mittal, M., and Mehta, A. 2008. Heavy metal induced oxidative stress and its possible reversal by chelation therapy. *Indian Journal of Medical Research*, 128:501-523.
- Gearheart, J. M., Clewell III, H. J., Crump, K. S., Shipp, A. M., and Silvers, A. 1995. Pharmacokinetic dose estimates of mercury in children and dose-response curves of performance tests in a large epidemiological study. *Water, Air, and Soil Pollution*, 80, 49- 58.
- Hadad, S., Beliveau, M., Tardiff, R., and Krishnan, K. 2001. A pbpk modelling based approach to account for interactions in the health risk assessment of chemical mixtures. *Toxicological Science*, 63: 125-131.
- Hadad, S. and Krishnan, K. 1998. Physiological modelling of toxicokinetic interactions: Implications for mixture risk assessment. *Environmental Health Perspectives*, 106(6):1377-1384.
- Krishnan, K., Clewell III, H. and Andersen, M. 1994. Physiologically based pharmacokinetic analysis of simple mixtures. *Environmental Health Perspectives*, 102(9):151-155.
- Mumtaz, M., Fisher, J., Blount, B., and Ruiz, P. 2013. Application of physiologically based pharmacokinetic models in chemical risk assessment. *Journal of Toxicology*, 2012:1-11.
- O'Flaherty, E. J. 1993. Physiologically based models born-seeking elements IV: Kinetics of lead disposition in humans. *Toxicology and Applied Pharmacology*, 118:16-29.
- Ralston, N. V. C. 2008. Selenium health benefit values as seafood safety criteria. *EcoHealth*, 5:442-455.
- Ralston, N. V. C., Ralston, C. R., Blackwell III, J. L., and Raymond, L. J. 2008. Dietary and tissue selenium in relation to methylmercury toxicity. *NeuroToxicology*, 890:1-10.
- Ralston, V. C. and Raymond, L. J. 2008. Jv Task 96-phase 2- investigating the importance of the mercury-selenium interaction. Technical Report, University of North Dakota.
- Raymond, L. and Ralston, N. V. C. 2004. Mercury:selenium interactions and health implications. *Seychelles Medical and Dental Journal*, 7(1):72-77.
- Ruiz, P., Ray, M., Fisher, J., and Mumtaz, M. 2011. Development of a human physiologically based pharmacokinetic (pbpk) toolkit for environmental pollutants. *International Journal of Molecular Science*, 12, 7469-7480.
- Shipp, A. M., Gentry, P. R., Lawrence, G., Landingham, C. V., Covington, T., Clewell, H.J., Gribben, K., and Crump, K. 2000. Determination of a site-specific reference dose for methyl mercury for fish-eating population. *Toxicology and Industrial Health*, 16:335-438.
- Silins, I. and Hogberg, J. 2011. Combined toxic

- exposures and human health: Biomarkers of exposure and effect. *International Journal of Environmental Research and Health*, 8:629-647.
- US Air Force, 2005. Physiologically-based pharmacokinetic/toxicokinetic modelling in risk assessment. Technical Report, United States Air Force Research Laboratory.
- US Environmental Protection Agency, 2006. Approaches for the application of physiologically based pharmacokinetic (pbpk) models and supporting data in risk assessment. National Center for Environmental Assessment, Washington DC; EPA/600/R-05/043F.
- Yoon, M., Schroeter, J. D., Nong, A., Taylor, M. D., Dorman, D. C., Andersen, M. E., and Clewell III, H. J. 2011. Physiologically based pharmacokinetic modelling effect of fetal and neonatal manganese exposure in humans: Describing Manganese homeostasis during development. *Toxicological Science*, 122(2): 297-316.
- Zhang, H. 2014. Impacts of Selenium on the Biogeochemical of cycles of Mercury in Terrestrial Ecosystems in Mercury Mining Areas. PhD Thesis, University of Chinese Academy of Science (formerly Graduate University of Chinese Academy), Beijing, China.